Inclusive eta photoproduction in nuclei

R. C. Carrasco
Institut für Kernphysik, Universität Mainz, D-6500 Mainz, Germany
(Received 19 March 1993)

A local model for the nuclear medium modifications to the photoproduction of η mesons through the $N^*(1535)$ resonance is applied to the study of the inclusive reaction in medium and heavy nuclei. The use of effective Lagrangians and many body quantum theory allows one to incorporate the nuclear decay channels of the N^* involving a pair of nucleons and Fermi sea effects. Also the ηN final state interaction is considered, taking into account the nuclear renormalization of the ηN scattering cross section, and assuming a classical propagation between collisions. The results show a depletion and broadening of the resonant shape. Total and differential cross sections for different nuclei are presented, and the cross section around resonance is found to behave like A^α with $\alpha \simeq 0.6$.

PACS number(s): 25.20.Lj, 13.60.Le

I. INTRODUCTION

The advent of high-duty-cycle electron accelerators and new experimental facilities (Mainz, Bonn, CEBAF, etc.) are expected to provide new and high quality data about η photoproduction on nucleons and nuclei, improving our present understanding of the η dynamics. The fact that the ηN interaction, in the region of invariant mass, 1400–1700 MeV is essentially driven by the $S_{11}(1535;\frac{1}{2}^-)$ reduces the overlap with other resonances and will help to extract information on the medium renormalization of this resonance. For this purpose, reactions induced by photons are especially suitable, because photons explore the whole nuclear volume.

Some theoretical work has already been done in order to describe the elementary amplitudes of processes involving eta mesons. Bennhold and Tanabe [1] derived a dynamical model for η photoproduction on nucleons by fitting the elementary operators to the $\pi N \to \pi N$, $\pi N \to \pi\pi N$, and $\pi N \to \eta N$ reactions and using the pion photoproduction reactions to parametrize the electromagnetic vertex. In a more recent work Tiator *et al.* [2] improved the model by adding Born terms to the elementary production amplitude.

The work of Liu and collaborators [3–5] used effective vertices to describe the η interaction with hadrons and focused on the question of detecting η nuclear bound states. In the last of these papers [5], they conclude that the widths of the bound states are rather large and its experimental detection difficult.

Also effective Lagrangians were used by Benmerrouche and Mukhopadhyay [6]. They found dominance of the resonant excitation in the (γ,η) reaction, and their analysis gave a value for the $\gamma N \to N^*(1535)$ helicity transition amplitude $A_{1/2} = (95\pm11)\times10^{-3}$ GeV$^{-1/2}$, compatible with theoretical estimates in quark models and also with the values extracted from pion photoproduction [7] (74 ± 11 in the same units). Compared to other methods, this effective Lagrangian approach reduces the number of parameters to be fitted and, thus, the uncertainties stemming from the experimental data.

In Ref. [1], coherent nuclear cross sections within the (DWIA) distorted wave impulse approximation were calculated, and they were found to be small. Indeed, relatively large momentum transfers are involved in (γ,η) — larger than in the (γ,π^0) case— and the form factors suppress the cross section by several orders of magnitude. Furthermore, the isoscalar photoexcitation of the S_{11} resonance seems to be very small compared to the isovector one [7]. Therefore, the coherent (γ,η) reactions are difficult to investigate experimentally. However, in inclusive processes, the contribution of each nucleon adds incoherently and the cross sections should be larger. Thus, a study of the main nuclear medium effects on the η photoproduction, suitable for the description of this reaction in medium and heavy nuclei, is of interest. It can also provide information about the free $n(\gamma,\eta)n$ cross section, which has not yet been measured. In this respect, the model of Refs. [1,2] gives a small ratio of isoscalar to isovector (γ,η) amplitudes, $E_{0+}^{(0)}/E_{0+}^{(1)} \simeq 0.25$, consistent with quark models, although larger values of this ratio seem necessary in order to explain the deuteron data [8]. Recent results from Mainz seem to indicate that this ratio might be indeed very small [9]. The origin of this discrepancy may come from two body currents. Indeed, when the momentum mismatch is large, two nucleons sharing this momentum makes the process more efficient. The contribution of many particles in η related processes has been shown in Ref. [10].

In this contribution, the many body calculations of the $N^*(1535)$ width of Ref. [5] for the case of bound η states are extended to the particular dynamics of η photoproduction and (η,η') rescattering, and applied to the calculation of the medium renormalization of these processes. In this sense, this work serves as a check of that model [5] for the S_{11} width, as found in the Appendix, in the case of (γ,η) inclusive processes. The role of other resonances or background terms will require additional work (even in order to clarify the situation in the free reactions), and here only the role of the S_{11} will be studied, as the other contributions to the free cross section in our energy domain are found to be small by the different

theoretical models [6,2].

The cross section for the reaction where the photon disappears exciting a $N^\star$ is calculated by means of the local density approximation (LDA). A detailed justification of the validity of this approximation in photonuclear reactions can be found in Ref. [11]. There it was proven that, due to the negligible loss of photon flux in the reaction, the effects of the finite range of the interaction do not lead to changes in the LDA prescription. On the other hand, shadowing effects due to the interference with the coherent ρ photoproduction are known to be visible only at higher energies ($\omega \simeq 2$ GeV), and should be negligible in the η channel, due to the weak coupling of the ρ to the S_{11} resonance. However, the value given by the LDA is not the observable eta photoproduction cross section, because of the η-nucleus final state interaction. The on-shell propagation of the η and its final state interaction are considered by means of a Monte Carlo (MC) program which makes use of the quantum mechanically calculated reaction probabilities. These MC methods provide a reliable treatment of the final state interaction in inclusive photonuclear reactions, as proven in the case of pions [12] and nucleons [13]. The complexity of these multistep problems, which involve strongly interacting particles, cannot be considered by a simple attenuation from distortion. Indeed, some of the particles are rescattered; they change energy and momentum, but they are not removed from the flux, and one should keep track of them. A partial justification of these MC methods can be found in Ref. [14], where the quantum mechanical reaction cross section for pion nuclear reactions and the one obtained from the MC method were found to agree within 5% for pions with $p_\pi > 200$ MeV. Thus, one expects also a reasonable description of η rescattering, provided that the outgoing momentum is not very small. The works of Refs. [14,12] also give support to the Fermi gas model assumed here. The Fermi gas model for inclusive reactions was found to provide fair cross sections and angular and energy distributions for inclusive reactions, except for slightly narrow energy distributions around the quasielastic peek in (π,π') [14]. This drawback of the model was not so evident in (γ,π) inclusive reactions [12].

With this method, the nuclear density is the only information needed about nuclear structure, and the treatment of heavy nuclei is not more difficult than the one of lighter nuclei. The basic ingredients for the elementary amplitudes in the model will be described in Sec. II, and the medium effects on the cross section are discussed in Sec. III. Finally, results and discussion will be presented in Sec. IV.

II. ETA PHOTOPRODUCTION ON THE NUCLEON

The model of Refs. [3–5] assumes the dominance of the $N^\star(1535;\frac{1}{2}^-)$ resonance for the ηN interaction. This is the only resonance up the $N^\star(1700)$ with a significant branching ratio into the ηN channel (about 50%, while in the other resonances is below 1.5%). The $N^\star(1535)$ may decay into the ηN, πN or $\pi\pi N$ channels (Fig. 1), and the corresponding couplings are given by [5]

$$\delta H_{\eta N N^\star} = g_\eta \bar{\psi}_{N^\star} \psi_N \Phi_\eta + \text{H.c.}, \tag{1}$$

$$\delta H_{\pi N N^\star} = g_\pi \bar{\psi}_{N^\star} \boldsymbol{\Phi}_\pi \boldsymbol{\tau} \psi_N + \text{H.c.}, \tag{2}$$

$$\delta H_{\pi\pi N N^\star} = -iC \bar{\psi}_{N^\star} \gamma^5 \psi_N \boldsymbol{\Phi}_\pi \boldsymbol{\Phi}_\pi + \text{H.c.} \tag{3}$$

The coupling constants are fixed in order to reproduce the $p(\pi^-,\eta)n$ experimental data [15], together with the $N^\star$ branching ratios [7], leading to

$$g_\pi = 0.564, \quad g_\eta = 1.613, \quad C = 7.14 m_\pi^{-1}. \tag{4}$$

The $N^\star$ mass is taken to be $M_{N^\star} = 1555$ MeV and $\Gamma(\sqrt{s} = M_{N^\star}) \simeq 110$ MeV, values lying within the experimental bounds. With the numbers of previous equation, one gets a fairly good cross section for $\pi N \to \eta N$ in the region of invariant mass, 1500–1600 MeV, with an accuracy of around 10%–15%. In order to study the η photoproduction, the electromagnetic vertex is also needed [6],

$$\delta H_{\gamma N N^\star} = -i\bar{\psi}_{N^\star} \gamma^5 \frac{e(\kappa_S + \kappa_V \tau_0)}{(M_N + M_{N^\star})} \sigma_{\mu\nu} \psi_N k^\mu \epsilon^\nu + \text{H.c.} \tag{5}$$

With this structure of the vertex, the amplitude is automatically gauge invariant (even if form factors are included), and its dominant contribution in (γ,η) has the structure of a E_{0+} transition,

$$T = e\, g_\eta \frac{\kappa^N}{M_N + M_{N^\star}} \boldsymbol{\sigma} \cdot \boldsymbol{\epsilon}\, G_{N^\star} \left(\omega_{\text{c.m.}} + \frac{\omega_{\text{c.m.}}^2}{2M_N} \right), \tag{6}$$

$\omega_{\text{c.m.}}$ being the center of mass photon energy and $G_{N^\star}$ the resonance propagator,

$$G_{N^\star} = \frac{1}{\sqrt{s} - M_{N^\star} + i\frac{\Gamma}{2}}. \tag{7}$$

Expressions for the free width with the couplings of Eqs. (1)–(3) can be found in the Appendix. The dominance of this E_{0+} multipole in the free (γ,η) cross section is well known, both from experimental [16,17] and theoretical analyses [1,2,6]. Finally, the elementary cross section in the c.m. frame is given by

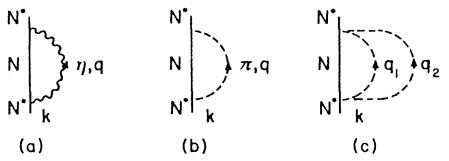

FIG. 1. Contributions to the $N^\star$ free width: (a) One eta decay channel. (b) One pion channel. (c) Two pion channel.

$$\frac{d\sigma}{d\Omega_{\rm c.m.}} = \frac{1}{16\pi^2}\frac{M^2}{s} g_\eta^2 |G_{N^\star}|^2 \left(e\kappa^N \frac{\omega_{\rm c.m.} + \frac{\omega_{\rm c.m.}^2}{2M_N}}{M_N + M_{N^\star}} \right)^2 . \tag{8}$$

A value of $\kappa^p = 0.86$ [6] gives a fair reproduction of the experimental data for the total cross section [17,18] and the E_{0+} multipole [19]. There are no experimental data for (γ,η) on the neutron. The isoscalar-isovector rate of 0.25 obtained from models based on multipole analysis [2] gives $\kappa^n = 0.52$. With these values, which are compatible with the helicity amplitudes for the electromagnetic transition $\gamma N \to N^\star(1535)$ reported by Particle Data Group [7], one obtains the elementary cross sections plotted in Fig. 2.

III. NUCLEAR MEDIUM EFFECTS

Inside the nucleus, new decay channels for the $N^\star$, such as those depicted in Fig. 3, are possible. They involve two nucleons exchanging virtual pions or η's. In order to calculate its contribution, one needs the πNN and ηNN couplings

$$\delta H_{\pi NN} = -i\frac{f_\pi}{m_\pi} 2M_N \bar\psi_N \gamma^5 \mathbf{\Phi}_\pi \cdot \boldsymbol{\tau} \psi_N F_\pi(q^2), \tag{9}$$

$$\delta H_{\eta NN} = -i\frac{f_\eta}{m_\pi} 2M_N \bar\psi_N \gamma^5 \psi_N \Phi_\eta F_\eta(q^2), \tag{10}$$

where form factors of the monopole type are included, $F(q^2) = \frac{\Lambda^2 - m^2}{\Lambda^2 - q^2}$. The values of the coupling constants and range of form factors are taken from Ref. [20]:

$$f_\eta = 0.59, \quad f_\pi = 1.0, \quad \Lambda_\eta = 1.5 \text{ GeV}, \quad \Lambda_\pi = 1.3\,\text{GeV}. \tag{11}$$

The coupling constant f_π is well established. The value of f_η is not so well known, but the different analysis of Refs. [20,21] coincide with the value taken here. Λ_η is taken from Bonn potential, and we will assume $\Lambda_\eta \simeq \Lambda_\eta$ with not much support. Given the momentum transfers involved in these absorption processes, the results depend only moderately on the detailed structure of the form factors.

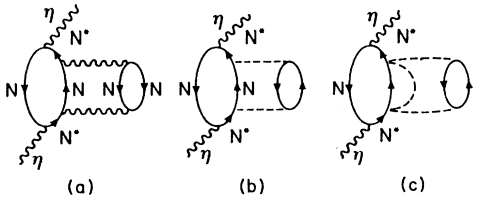

FIG. 3. Eta self-energy diagrams in nuclear matter corresponding to two body absorption modes. The corresponding eta-absorption channel is obtained when the diagrams are cut by a horizontal line.

With these ingredients, simple expressions for the effective width in nuclear matter, $\Gamma_{\rm eff}$, can be obtained (see the Appendix or Ref. [5] for details). The contribution of every decay channel to the width is separately given by the model, as seen in Fig. 4. In order to calculate the nuclear cross section, one should also consider the Fermi motion of the nucleons, together with the Pauli blocking in the Fermi sea. This is easily accomplished by means of the expression

$$\sigma = \int d\mathbf{r}\; 4 \int \frac{d\mathbf{p}}{(2\pi)^3} n(\mathbf{p}) \int d\Omega_{\rm c.m.} \frac{d\sigma}{d\Omega_{\rm c.m.}}(\sqrt{s}) \times \Theta[\kappa - \hat{\mathbf{P}}\cdot\hat{\mathbf{q}}_\eta] \frac{\sqrt{s}\,\omega_{\rm c.m.}}{\omega E_N}, \tag{12}$$

where $P^\mu = (P^0, \mathbf{P})$ is the $N^\star$ four-momentum, $s = P_\mu P^\mu$, and E_N the nucleon energy in the Fermi sea. The differential cross section $d\sigma/d\Omega$ in Eq. (12) is given by

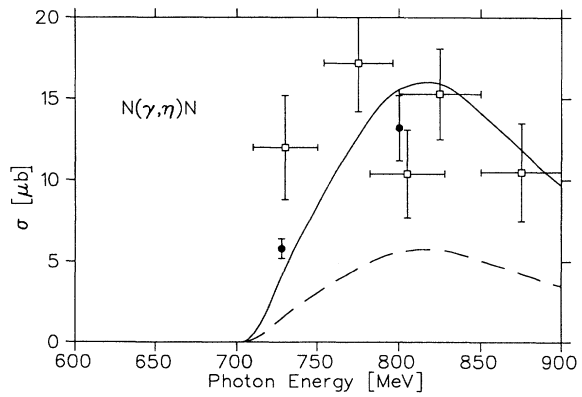

FIG. 2. Elementary (γ,η) cross sections, on the proton (solid curve) and neutron (dashed curve). Experimental data for the proton from Refs. [18] (○) and [17] (●).

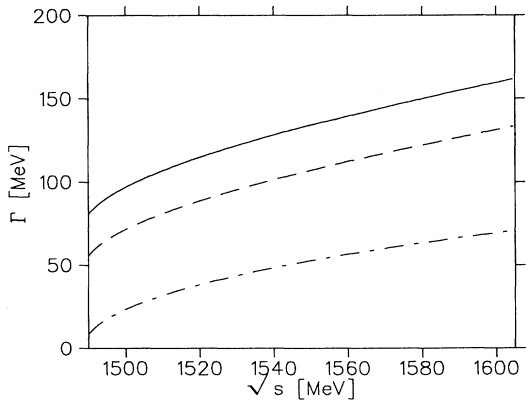

FIG. 4. $N^\star$ width acording to Ref. [5], as a function of the invariant mass (the kinematics correspond to those of the free γN reaction). Dash-dotted curve: quasielastic channel. Dashed curve: free width (quasielastic plus one or two pion decay). Solid curve: free plus absorptive width at $\rho = \rho_0$.

Eq. (8), where the $N^\star$ width has been replaced by $\Gamma_{\rm eff}$ in the medium. The last factor in Eq. (12) comes from the different definition of the flux in the c.m. frame and the nucleus at rest frame. The integral over the momenta takes proper account of the Fermi motion, while the step function implements the Pauli blocking as a restriction to the center of mass scattering angles. The value of κ is given by

$$\kappa = x\Theta(1-|x|) + \frac{x}{|x|}\Theta(|x|-1), \tag{13}$$

$$x = \frac{P^0 p^0_{\rm c.m.} - \epsilon_F\sqrt{s}}{|\mathbf{P}||\mathbf{p}_{\rm c.m.}|}, \tag{14}$$

where $(p^0_{\rm c.m.}, \mathbf{p}_{\rm c.m.})$ is the outgoing nucleon momentum in the c.m. frame, and ϵ_F is the Fermi energy.

Equation (12) gives the nuclear cross section prior to the final state interaction. Even if created, some η's will rescatter or disappear before leaving the nucleus. The integrand in Eq. (12) represents the weight of the different events. In other words, it gives the spatial distribution inside the nucleus and the probability that the η is generated at a given scattering angle. This is used as input of the MC code, which allows one to take account of the final state interaction. For this purpose, one needs the η mean free path in the nucleus, related to the imaginary part of the η self-energy in the medium,

$$\frac{1}{\lambda} = -\frac{1}{q_\eta}\,{\rm Im}\,\Pi(q_\eta,\rho) = -\frac{1}{q_\eta}g_\eta^2\,4\int\frac{d\mathbf{p}}{(2\pi)^3}n(\mathbf{p})\,{\rm Im}\,G_{N^\star}. \tag{15}$$

The imaginary part of the propagator is simply

$${\rm Im}\,G_{N^\star} = -\frac{\frac{\Gamma_{\rm eff}}{2}}{|\sqrt{s} - M_{N^\star} + i\frac{\Gamma_{\rm eff}}{2}|^2}. \tag{16}$$

In this way, the effects of the Fermi motion and the changes in the $N^\star$ width are automatically incorporated. The change of the $N^\star$ mass in the nuclear medium, i.e., the real part of the $N^\star$ self-energy, remains an open question. Here, the same strength for the $N^\star$ potential and the N potential were assumed (${\rm Re}\,\Sigma_N = -50\rho/\rho_0$), leading to an unshifted resonance mass in the propagator $G_{N^\star}$. On the other hand, the effective width consists of different pieces, stemming from the contribution of the different channels ($\Gamma_{\rm eff} = \Gamma_\eta + \Gamma_\pi + \Gamma_{\pi\pi} + \Gamma_{\rm abs}$) and one can separate the quasielastic channel by taking only Γ_η in the numerator of Eq. (16). Thus, $\Gamma_\eta/\Gamma_{\rm eff}$ gives the reaction probability associated with quasielastic collisions, the remainder corresponding to η absorption (in the sense that the η disappears, producing particle-hole excitations and occasionally pions). The probabilities that the η disappears (via absorption or pion production) or rescatters are evaluated at every step in the MC simulation code. In this way, even multiple collisions of the outgoing η are taken in to account. Collisions change its energy and momentum, and the code traces the η until it is absorbed or leaves the nucleus.

IV. RESULTS AND DISCUSSION

Figures 5 and 6 show the η inclusive photoproduction cross sections per nucleon in the case of ^{16}O and ^{208}Pb, respectively, compared to the impulse approximation (upper curve). The intermediate curve is the nuclear cross section, including changes of the $N^\star$ width, Fermi motion, and Pauli blocking effects. Finally, the lower one incorporates the final state interaction of the η. Due to the Fermi motion of the nucleons, a certain amount of η's can be produced, below the production threshold on the free nucleon ($\omega_{\rm th} \simeq 710$ MeV). This effect is not seen in pion photoproduction close to threshold ($\omega_{\rm th} \simeq 150$ MeV). Indeed, while Pauli blocking effects are very important for low energy pions, they are very small for low energy η's, because the momenta transferred to the nucleon in η photoproduction are much larger. This is also the reason for the relatively small modification of the $N^\star$ free decay width in the nuclear medium. However, the absorption channels, which are genuine nuclear channels, increase the width and the resonant shape is broadened and depleted. The decrease in the maximum value can be easily seen from Eqs. (7) and (8), as close to the resonance the propagator is roughly proportional to $1/\Gamma_{\rm eff}$. The effect is analogous—although in a different energy regime—to the well known change of the Δ resonance shape in nuclei.

The cross section per nucleon should approach the impulse approximation as the number of nucleons A decreases. Thus, the depletion is more important in heavier nuclei. It may look contradictory that a roughly constant cross section per nucleon is found in the Δ resonance region [22]. However, the same kind of behavior is found, once the important direct absorption channels are subtracted [11].

Obviously, the effect of the final state interaction also increases in heavier nuclei, because an average η covers longer distances inside the nucleus. As a result, about 65% of the η's are absorbed before leaving ^{208}Pb, and

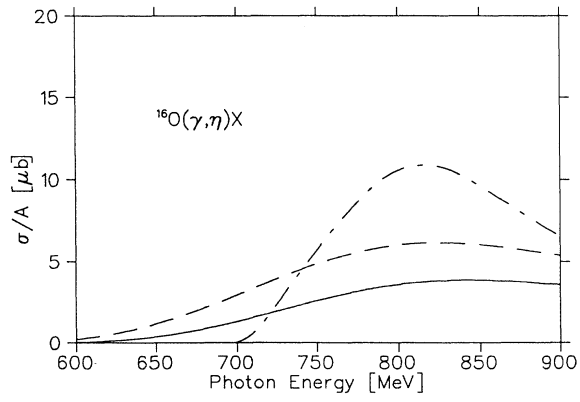

FIG. 5. Inclusive eta photoproduction cross section on ^{16}O. Dash-dotted curve: impulse approximation. Dashed curve: modifications due to the Fermi sea and nuclear S_{11} width. Solid curve: complete calculation, including final state interaction.

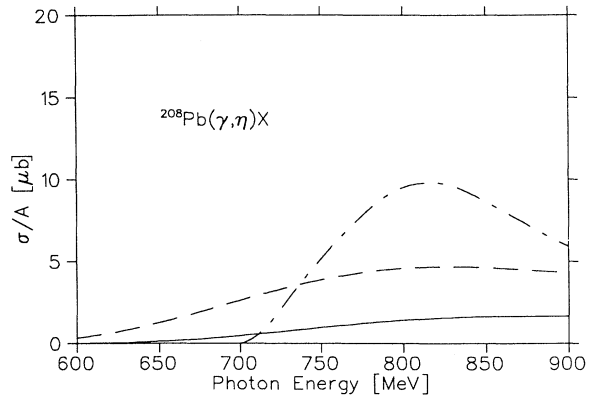

FIG. 6. Same as Fig. 4, for ^{208}Pb.

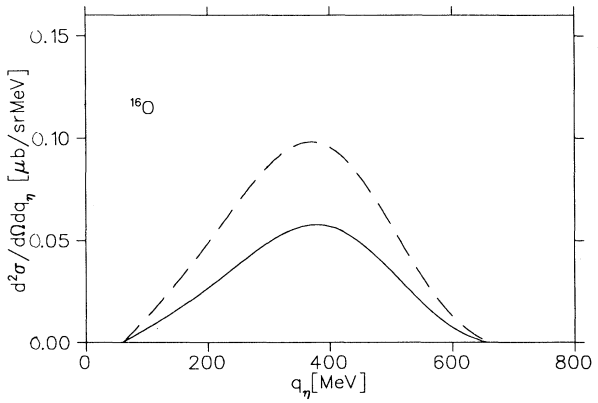

FIG. 8. Differential cross section $\frac{d^2\sigma}{d\Omega dq_\eta}$ (μb/sr MeV) at scattering angle $\Theta = 25°$ and photon energy ω =800 MeV for ^{16}O. Dashed curve: without final state interaction. Solid curve: after final state interaction.

only about 40% in the case of ^{16}O. The number of observed η's which have been rescattered before leaving the nucleus is about 13% and 9%, respectively. Clearly, the final state interaction is by no means negligible and leads to significant differences in the cross sections. Figure 7 shows that the cross section at $\omega = 800$ MeV grows as A^α with $\alpha \simeq 0.6$. This behavior is similar to that of pions around the Δ resonance energy, which give $\alpha \simeq 0.65$ [23], and reflects the fact that particles produced deep inside the nucleus have only a small chance to escape, together with the fact that medium renormalization is stronger at higher densities, and therefore the creation probabilities are smaller.

Figures 8 and 9 show differential cross sections $(d^2\sigma/d\Omega dq_\eta)$, before and after the final state interaction (the impulse approximation would give a delta function). Changes in the shape of these distributions due to the final state interactions are not so strong as the effects on the size of the total cross section.

Finally, let us consider the importance of the inclusive process (γ,π) followed by (π,η). Indeed, the (γ,π) cross sections are bigger than the (γ,η) ones (about a factor 5 for charged pion production [24]). However, the (π^+,η) cross section is given by

$$\frac{d\sigma}{d\Omega_{\rm c.m.}} = \frac{1}{16\pi^2}\frac{M^2}{s}2g_\eta^2 g_\pi^2 \frac{q_\eta}{q_\pi}|G_{N^*}|^2. \qquad (17)$$

The (η,η') cross section has the same structure, but it does not contain the factor 2 of isospin, and g_η and q_η replace g_π and q_π, respectively. Thus, at a given value of $\sqrt{s} \simeq 1555$ MeV one gets a factor of one-tenth between the (π,η) and (η,η) cross sections. This fact, together with the low rate of rescattering (about 10%) previously quoted, suggests a very small contribution from this source (below 5%).

V. CONCLUSIONS

The inclusive η photoproduction cross section through the $N^*(1535)$ has been studied by means of a local model which allowed one to incorporate the medium modifications of the $N^*(1535)$ decay width and Fermi sea effects, as well as final state interactions of the photoproduced

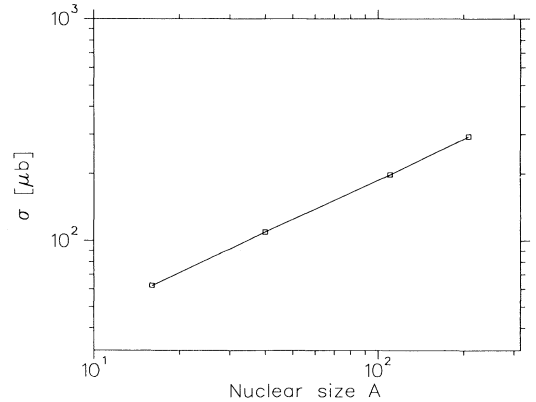

FIG. 7. Dependence of the total cross section at $\omega = 800$ MeV on the nuclear mass number A.

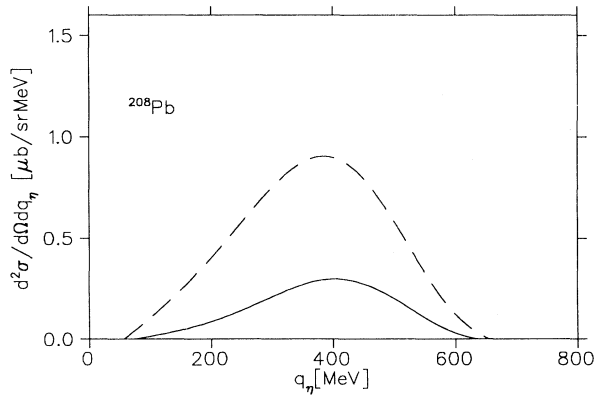

FIG. 9. Same as Fig. 8, for ^{208}Pb.

η's. The calculations show that both final state interaction and medium renormalization of the cross section are important at the energies of the S_{11}. Similar analyses should be performed for the other resonances in order to have a complete description of the nuclear processes in the second resonance region. The results show a strong depletion of the resonant shape, particularly in heavier nuclei, and the cross section is found to grow as A^α with $\alpha \simeq 0.6$. Measurements of the inclusive (γ,η) cross section will provide information about the renormalization of the S_{11} response. They will also check the pole position of the resonance in the nucleus, as well as the isospin dependence of the (γ,η) process, which is still controversial. The present model also provides the energy distribution and differential cross sections for the outgoing η's, which may be quite useful for future experimental analyses. With the present experimental facilities at Mainz, the results showed in Figs. 5–9 could be tested experimentally.

ACKNOWLEDGMENTS

I would like to thank E. Oset and S. S. Kamalov for useful discussions, and suggestions from D. Drechsel, L. Tiator, and N. C. Mukhopadhyay. This work was supported by Spanish Ministerio de Educacion y Ciencia.

APPENDIX: N^* WIDTH IN NUCLEAR MATTER

The calculation of the resonant width follows the model of Ref. [5]. The expressions for different contributions to the free width are

$$\frac{\Gamma_\pi}{2} = 3\,\frac{g_\pi^2}{4\pi}\,\frac{M}{\sqrt{s}}\,q_\pi^{\rm c.m.}, \tag{A1}$$

$$\frac{\Gamma_\eta}{2} = \frac{g_\eta^2}{4\pi}\,\frac{M}{\sqrt{s}}\,q_\eta^{\rm c.m.}, \tag{A2}$$

$$\frac{\Gamma_{\pi\pi}}{2} = 6\left(\frac{C}{8M_{\rm red}}\right)^2 \frac{M}{(2\pi)^3} \times \int_{m_\pi}^{E_{\rm max}} dE_2 \int_{m_\pi}^{\sqrt{s}-M-E_2} dE_1\, p_N^2\,\Theta(1-|\beta|), \tag{A3}$$

where

$$M_{\rm red} = M_N M_{N^*}/(M_N + M_{N^*}),$$

$$E_{\rm max} = \frac{(s - M^2 - 2Mm_\pi)}{2\sqrt{s}},$$

and

$$\beta = \frac{1}{2q_1q_2}[s + 2m_\pi^2 - M^2 - 2\sqrt{s}(E_1+E_2) + 2E_1E_2]. \tag{A4}$$

The diagrams of Fig. 3 were evaluated in Ref. [5] by using Cutkosky rules [25] and a useful approximation for the contribution of the particle-hole loop [26],

$$\Theta(q^0)\,{\rm Im}\,U_N(q) \simeq -\pi\rho\delta(q^0 - q^2/2M),$$

and the results are

$$\frac{\Gamma_\pi^{\rm abs}}{2} = 3\frac{g_\pi^2}{4\pi}\frac{f_\pi^2}{m_\pi^2}\rho M q_t^3 \frac{F_\pi^4(q_t^0,q_t)}{(q_t^{02} - q_t^2 - m_\pi^2)^2}, \tag{A5}$$

$$\frac{\Gamma_\eta^{\rm abs}}{2} = \frac{g_\eta^2}{4\pi}\frac{f_\eta^2}{m_\pi^2}\rho M q_t^3 \frac{F_\eta^4(q_t^0,q_t)}{(q_t^{02} - q_t^2 - m_\eta^2)^2}, \tag{A6}$$

$$\frac{\Gamma_{\pi\pi}^{\rm abs}}{2} = 6\left(\frac{C}{4M_{\rm red}}\right)^2 \frac{\rho}{(2\pi)^3}\frac{f_\pi^2}{m_\pi^2}\int_0^{q_{2\rm max}} dq_2 \int_0^{q_{1\rm max}} dq_1\, q_1^3 q_2\,\Theta(1-|\beta|) \times (2Mk^0 - q_1^2 - k^2 - 2ME_2)\frac{M}{E_2}\frac{F_\pi^4(q_1^0,q_1)}{(q_1^{02} - q_1^2 - m_\pi^2)^2} \tag{A7}$$

where $q_t = \sqrt{Mk^0 - k^2/2}$, $q_t^0 = q_t^2/2M$, $q_{2\rm max} = \sqrt{4Mk^0 - 2k^2 - 4Mm_\pi}$, $q_{1\rm max} = (q_2 + \sqrt{q_{2\rm max}^2 - q_2^2})/2$, $q_1^0 = q_1^2/2M$, and $(k^0 + M)$ is the N^* energy and k its momentum, and

$$\beta = \frac{M}{q_1q_2}\left(k^0 - \frac{k^2}{2M} - \frac{q_1^2}{M} - \frac{q_2^2}{2M} - E_2\right). \tag{A8}$$

[1] C. Bennhold and H. Tanabe, Nucl. Phys. **A530**, 625 (1991).

[2] L. Tiator, S.S. Kamalov, and C. Benhold, invited talk to the National Conference on Physics of Few Body and Quark-Hadronic Systems, Kharkov, Ukraine, 1992 (unpublished).

[3] R.S. Bhalerao and L.C. Liu, Phys. Rev. Lett. **54**, 865 (1985).

[4] Q. Haider and L.C. Liu, Phys. Lett. B **172**, 257 (1986).
[5] H.C. Chiang, E. Oset, and L.C. Liu, Phys. Rev. C **44**, 783 (1991).
[6] M. Benmerrouche and N.C. Mukhopadhyay, Phys. Rev. Lett. **67**, 1070 (1991).
[7] Particle Data Group, Phys. Rev. D **45**, S1 (1992), Vol. 11-II.
[8] R.L. Anderson and R. Prepost, Phys. Rev. Lett. **23**, 46 (1969).
[9] B. Krusche (private communication).
[10] L.C. Liu, Phys. Lett. B **288**, 18 (1972).
[11] R.C. Carrasco and E. Oset, Nucl. Phys. **A536**, 445 (1992).
[12] R.C. Carrasco, E. Oset, and L.L. Salcedo, Nucl. Phys. **A451**, 585 (1992).
[13] R.C. Carrasco, M.J. Vicente, and E. Oset, Nucl. Phys. (submitted).
[14] L.L. Salcedo *et al.*, Nucl. Phys. **A484**, 557 (1988).
[15] R.M. Brown *et al.*, Nucl. Phys. **B153**, 89 (1979).
[16] B. Delcourt *et al.*, Phys. Lett. **29B**, 75 (1967).
[17] S.A. Dytman *et al.*, Bull. Am. Phys. Soc. **35**, 1679 (1990).
[18] S.I. Alekhin *et al.*, Report No. CERN-HERA 87-01, 1987 (unpublished).
[19] R.A. Arndt *et al.*, Phys. Rev. C **42**, 1853 (1990).
[20] R. Machleidt, K. Holinde, and Ch. Elster, Phys. Rep. **149**, 1 (1987).
[21] G.E. Brown and A.D. Jackson, *The Nucleon Nucleon Interaction* (North-Holland, Amsterdam, 1976).
[22] J. Ahrens *et al.*, Nucl. Phys. **A490**, 655 (1988).
[23] J. Arends *et al.*, Nucl. Phys. **A526**, 479 (1991).
[24] T. Fujii *et al.*, Nucl. Phys. **B120**, 395 (1977).
[25] C. Itzykson and J.B. Zuber, *Quantum Field Theory* (McGraw-Hill, New York, 1980).
[26] C. Garcia-Recio, E. Oset, and L.L. Salcedo, Phys. Rev. C **37**, 194 (1988).